Z. Phys. C – Particles and Fields 49, 225–233 (1991)

Zeitschrift für Physik C Particles and Fields

Measurement of π^0 and η meson production in e^+e^- annihilation at $\sqrt{s}$ near 10 GeV

Crystal Ball Collaboration

Ch. Bieler[8], D. Antreasyan[9], H.W. Bartels[5], D. Besset[11], J.K. Bienlein[5], A. Bizzeti[7], E.D. Bloom[12], I. Brock[3], K. Brockmüller,[5], R. Cabenda[11], A. Cartacci[7], M. Cavalli-Sforza[2], R. Clare[12], A. Compagnucci[7], G. Conforto[7], S. Cooper[a,12], R. Cowan[11], D. Coyne[2], A. Engler[3], K. Fairfield[12], G. Folger[6], A. Fridman[b,12], J. Gaiser[12], D. Gelphman[12], G. Glaser[6], G. Godfrey[12], K. Graaf[8], F.H. Heimlich[7,8], F.H. Heinsius[8], R. Hofstadter[12], J. Irion[9], Z. Jakubowski[4], H. Janssen[10], K. Karch[5], S. Keh[13], T. Kiel[8], H. Kilian[13], I. Kirkbride[12], T. Kloiber[5], M. Kobel[6], W. Koch[5], A.C. König[10], K. Königsmann[c,13], R.W. Kraemer[3], S. Krüger[8], G. Landi[7], R. Lee[12], S. Leffler[12], R. Lekebusch[8], A.M. Litke[12], W. Lockman[12], S. Lowe[12], B. Lurz[6], D. Marlow[3], H. Marsiske[5,12], W. Maschmann[5,8], P. McBride[9], F. Messing[3], W.J. Metzger[10], H. Meyer[5], B. Monteleoni[7], B. Muryn[d,4], R. Nernst[8], B. Niczyporuk[12], G. Nowak[4], C. Peck[1], P.G. Pelfer[7], B. Pollock[12], F.C. Porter[1], D. Prindle[3], P. Ratoff[1], M. Reidenbach[10], B. Renger[3], C. Rippich[3], M. Scheer[13], P. Schmitt[13], J. Schotanus[10], J. Schütte[6], A. Schwarz[12], D. Sievers[8], T. Skwarnicki[5], V. Stock[8], K. Strauch[9], U. Strohbusch[8], J. Tompkins[12], H.J. Trost[5], B. van Uitert[12], R.T. Van de Walle[10], H. Vogel[3], A. Voigt[5], U. Volland[6], K. Wachs[5], K. Wacker[12], W. Walk[10], H. Wegener[6], D.A. Williams[9,2], P. Zschorsch[5]

[1] California Institute of Technology, Pasadena, CA 91125, USA
[2] University of California at Santa Cruz[f], Santa Cruz, CA 95064, USA
[3] Carnegie-Mellon University[g], Pittsburgh, PA 15213, USA
[4] Cracow Institute of Nuclear Physics, PL-30055 Cracow, Poland
[5] Deutsches Elektronen Synchrotron DESY, W-2000 Hamburg, Federal Republic of Germany
[6] Universität Erlangen-Nürnberg[h], W-8520 Erlangen, Federal Republic of Germany
[7] INFN and University of Firenze, I-50125 Firenze, Italy
[8] Universität Hamburg, I. Institut für Experimentalphysik[i], W-2000 Hamburg, Federal Republic of Germany
[9] Harvard University[k], Cambridge, MA 02138, USA
[10] University of Nijmegen and NIKHEF[l], 6525 ED Nijmegen, The Netherlands
[11] Princeton University[m], Princeton, NJ 08544, USA
[12] Department of Physics[n], HEPL, and Stanford Linear Accelerator Center[o], Stanford University, Stanford, CA 94305, USA
[13] Universität Würzburg[p], W-8700 Würzburg, Federal Republic of Germany

Received 25 July 1990

[a] Present address: Max-Planck-Institut für Physik, W-8000 München 40, FRG
[b] Permanent address: DPHPE, Centre d'Etudes Nucléaires de Saclay, F-91191 Gif sur Yvette, France
[c] Present address: CERN, CH-1211 Genève 23, Switzerland
[d] Permanent address: Institute of Physics and Nuclear Techniques, AGH, PL-30055 Cracow, Poland
[e] Supported by the U.S. Department of Energy, contract No. DE-AC03-81ER40050 and by the National Science Foundation, grant No. PHY75-22980
[f] Supported by the National Science Foundation, grant No. PHY85-12145
[g] Supported by the U.S. Department of Energy, contract No. DE-AC02-76ER03066
[h] Supported by the German Bundesministerium für Forschung und Technologie, contract No. 054ER12P
[i] Supported by the German Bundesministerium für Forschung und Technologie, contract No. 054HH11P(7) and by the Deutsche Forschungsgemeinschaft
[k] Supported by the U.S. Department of Energy, contract No. DE-AC02-76ER03064
[l] Supported by FOM-NWO
[m] Supported by the U.S. Department of Energy, contract No. DE-AC02-76ER03072 and by the National Science Foundation, grant No. PHY82-08761
[n] Supported by the U.S. Department of Energy, contract No. DE-AC03-76SF00326 and by the National Science Foundation, grant No. PHY81-07396
[o] Supported by the U.S. Department of Energy, contract No. DE-AC03-76SF00515
[p] Supported by the German Bundesministerium für Forschung und Technologie, contract No. 054WU11P(1)

Abstract. We present a study of inclusive π^0 and η production in e^+e^- annihilation at $\sqrt{s} \approx 10$ GeV. Our analysis is based on integrated luminosities of 46.2 pb^{-1} taken at the $\Upsilon(1S)$ resonance and 42.1 pb^{-1} taken in the neighboring continuum. We measure the inclusive π^0 and η spectra for direct $\Upsilon(1S) \to 3g$ decays and continuum processes $e^+e^- \to q\bar{q}$ and obtain the following mean particle multiplicities per event:

Continuum:

$\langle n_{\pi^0} \rangle = 3.64 \pm 0.21 \pm 0.36$ $\langle n_\eta \rangle = 0.22 \pm 0.04 \pm 0.03$

$\Upsilon(1S) \to 3g$:

$\langle n_{\pi^0} \rangle = 3.39 \pm 0.14 \pm 0.34$ $\langle n_\eta \rangle = 0.35 \pm 0.04 \pm 0.04$.

We compare our results with predictions of different fragmentation models and with other measurements performed in e^+e^- annihilation at similar center-of-mass energies.

1 Introduction

The formation of hadrons from partons, as produced for example in e^+e^- annihilation, takes place at distances too large to be calculated in QCD perturbation theory. Therefore to describe these processes one must rely on phenomenological fragmentation models [1–4]. The models can be tested by comparing their predictions with measurements of hadron energy spectra and particle multiplicities at different center-of-mass energies in e^+e^- annihilation.

We report on a study of π^0 and η production performed with the Crystal Ball detector at the DORIS II e^+e^- storage ring. Special emphasis is put on the comparison of quark fragmentation in the process $e^+e^- \to q\bar{q} \to hadrons$ to gluon fragmentation in $\Upsilon(1S) \to 3g \to hadrons$ decays, which some models predict to be different. In particular we compare our results with predictions of the Lund color string model [2], the Webber coherent parton shower model [3], and the Peterson-Walsh model [4].

2 Data analysis

2.1 Detector and data samples

The Crystall Ball detector has been described in detail elsewhere [5] and its properties are only briefly summarized here. The main part of the detector consists of a highly segmented, spherical NaI calorimeter covering 93% of 4π sr. The calorimeter is designed to measure the directions and energies of photons, electrons and positrons with good angular and energy resolution. A system of proportional tube chambers surrounding the beam pipe is used to track charged particles and to distinguish between photons and charged particles with high efficiency.

The data used in this analysis comprise 46.2 pb^{-1} of integrated luminosity taken at the $\Upsilon(1S)$ resonance and 12.5 pb^{-1} of nonresonant continuum data taken just below and above the $\Upsilon(1S)$ resonance at e^+e^- center-of-mass energies, $\sqrt{s}$, of 9.39 GeV and 9.98 GeV. For the analysis of η production we also use 29.6 pb^{-1} of continuum data accumulated below the $\Upsilon(4S)$ resonance at 10.52 GeV. The integrated luminosities were obtained by measuring the number of large angle Bhabha events.

The number of observed events N_{ev} for the continuum analyses were $N_{ev} = 44000 \pm 200$ for the π^0 analysis and $N_{ev} = 131000 \pm 400$ for the η analysis. For $\Upsilon(1S) \to 3g$, N_{ev} is calculated from the number of observed hadronic and luminosity events on the resonance and in the continuum, giving $N_{ev} = 369000 \pm 4000$ events, where the error is dominated by systematic uncertainties. The procedure used to determine the number of hadronic events is described in [6].

2.2 Particle identification and reconstruction

Hadronic events are selected from the raw data samples with selection criteria suited to suppress background from beam-gas and beam-wall reactions, two-photon collisions, and QED processes like e- and τ-pair production. The cuts used for the hadronic event selection are the same as those applied in our previous analysis of the inclusive electron spectrum in semileptonic B decays and are described in detail in [5].

The production of π^0 and η mesons in hadronic events is studied by reconstructing these mesons in their decay mode into two photons. Photons are measured with good energy resolution and leave a very symmetric lateral shower profile in the NaI crystals of the calorimeter, which allows an efficient identification by pattern recognition techniques.

For π^0 energies below 500 MeV the two decay photons are generally well-separated in the calorimeter. The π^0 can then be reconstructed from the energies and directions of the two photons. The π^0 mass resolution, $\sigma(\pi^0)$, depends on the photon energy and angle measurements and worsens with increasing π^0 energy. The resolution as a function of the π^0 energy is obtained from a Monte Carlo study and varies almost linearly from $\sigma = 8.2$ MeV/c^2 at 140 MeV to $\sigma = 16.2$ MeV/c^2 at 500 MeV.

For π^0 mesons of higher energy the energy deposits of the two photons frequently overlap forming just one cluster in the calorimeter. An efficient reconstruction of high energy π^0 mesons is performed by means of the second moment S of an energy cluster, defined as [7]

$$S = \frac{1}{E_c} \sum_i (\hat{n}_i - \hat{c})^2 E_i, \tag{1}$$

where E_i is the energy in the i^{th} crystal of the cluster and $\hat{n}_i$ is the unit vector pointing from the interaction point to the center of the crystal. The sum of energies of all crystals in the cluster is denoted by $E_c = \sum_i E_i$ and

$\hat{c}=\frac{1}{E_c}\sum_i \hat{n}_i E_i$ is the vector pointing to the center of gravity of the energy cluster. The second moment S is related to the shower mass M_S by

$$M_S = E_c\sqrt{|S-S_\gamma|}, \tag{2}$$

where S_γ denotes the average second moment of a single photon shower of energy E_c. S_γ is almost energy independent and is obtained from Monte Carlo calculations. For π^0 energies below about 1.6 GeV, showers from photons and π^0 mesons can be efficiently discriminated on a cluster-by-cluster basis by this method.

To reconstruct π^0 and η mesons in their two photon decay mode we search for photon candidates in each of our preselected hadronic events. Particles within $|\cos\vartheta|<0.85$, where ϑ is the polar angle with respect to the beam axis, are taken as photon candidates, if they are not identified as charged by the tracking chamber system. In addition the lateral shower pattern has to be consistent with that expected for a single electromagnetically showering particle and the shower mass M_S is required to be significantly below the π^0 mass value.

For each two-photon combination in the event the invariant mass and the total energy of the two-photon system are calculated. The resulting mass spectrum shows a striking π^0 signal. To study the π^0 yield as a function of the pion energy the two-photon invariant mass distributions are analyzed in bins of the scaled energy variable $z=2E_{\gamma\gamma}/\sqrt{s}$, where $E_{\gamma\gamma}$ is the total energy of the two-photon system. The full z range is divided into intervals of $\Delta z=0.02$. Mass distributions from continuum data for two z bins are shown in Figs. 1a, b. A reconstruction of π^0 mesons using the invariant mass method is achieved up to $E(\pi^0)\leqq 950$ MeV ($z\leqq 0.2$) with a steady decrease in efficiency for pion energies above 500 MeV. In contrast, the shower mass technique allows an efficient reconstruction of π^0 mesons of energies above

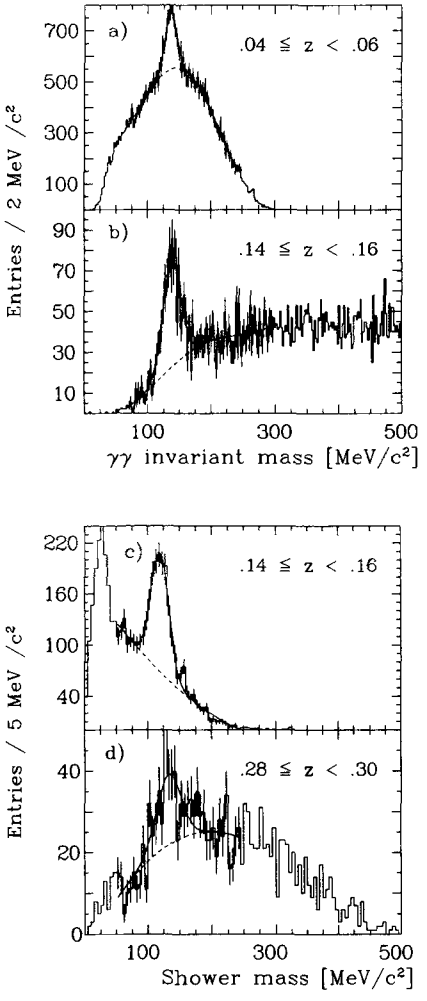

Fig. 1a–d. The $\gamma\gamma$ invariant mass spectra for continuum data in the π^0 mass region. Selected z bins are shown. The spectra of **a**, **b** were obtained with the invariant mass method, while **c**, **d** are obtained with the shower mass technique. The fit results for the π^0 signal (solid line) and the background (dashed line) are superimposed on the data

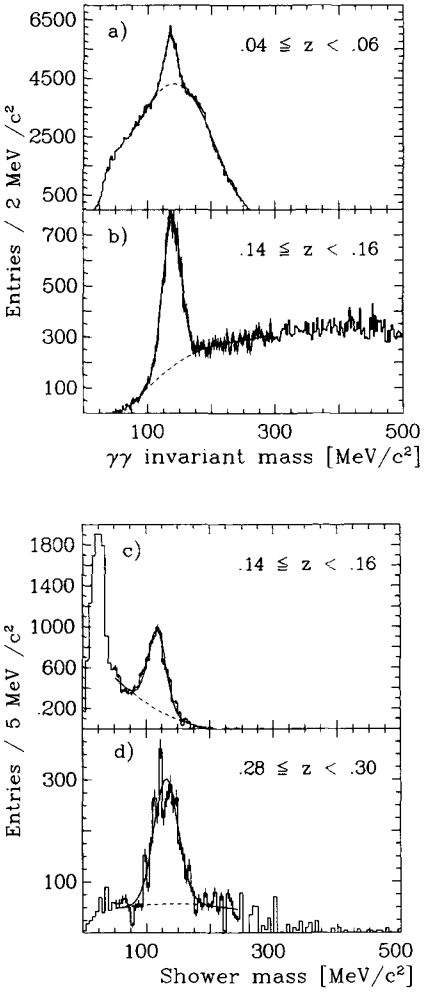

Fig. 2a–d. The $\gamma\gamma$ invariant mass spectra for $\Upsilon\to 3g$ events in the π^0 mass region. Selected z bins are shown. The spectra of **a**, **b** were obtained with the invariant mass method, while **c**, **d** are obtained with the shower mass technique. The fit results for the π^0 signal (solid line) and the background (dashed line) are superimposed on the data

about 700 MeV ($z \geqq 0.14$) up to 1.6 GeV ($z \leqq 0.34$). Distributions of the shower mass M_S are shown for continuum data in two z bins in Figs. 1c, d.

The corresponding distributions for $\Upsilon(1S) \to 3g$ events, shown in Fig. 2, are obtained for each z interval by subtracting the normalized continuum mass spectrum from the corresponding mass spectrum of the $\Upsilon(1S)$ resonance data. The normalization factor takes into account the luminosity ratio between the two data samples, the event selection efficiencies for $\Upsilon(1S) \to 3g$ and $\Upsilon(1S) \to q\bar{q}$ decays, and the branching ratio $B(\Upsilon(1S) \to q\bar{q})$.

By fitting the mass distributions, the number of reconstructed π^0 mesons is determined in each z interval of each sample. The π^0 signal is described by a Gaussian with a z-dependent width, which was obtained from a Monte Carlo study. The background shape was parametrized by fourth or second order polynomials, depending on whether the spectrum was obtained by the invariant mass method or the shower mass technique. The fit results are superimposed on the data shown in Fig. 1 and Fig. 2.

The study of η production is based on a larger continuum sample by using in addition 29.6 pb^{-1} of data taken just below the $\Upsilon(4S)$ resonance. Furthermore, due to poorer statistics the η production is analyzed in wider intervals of $\Delta z = 0.04$. The energy deposits of the two photons from $\eta \to \gamma\gamma$ seldom overlap in the calorimeter. Accordingly we restrict the analysis to the reconstruction of η mesons from two well-separated photons. However, the analysis suffers from a large combinatoric background in the η mass region. A reduction of the combinatoric background below the η signal is achieved with an algorithm to suppress photons from π^0 decays. The algorithm selects that combination of photon pairs which yields the largest number of invariant masses compatible with the π^0 mass. The photons forming these π^0 candidates are ignored. The remaining photons in the event are then paired, revealing an η signal. Figure 3 shows the resulting two-photon invariant mass spectra for the continuum data and the $\Upsilon(1S) \to 3g$ events. The highest z interval for which the η signal is fitted is [0.40–0.44]. The fits assume a Gaussian shape for the signal with a fixed mass resolution of $\sigma(\eta) = 25$ MeV/c^2, constant for all z intervals, plus a background described by third order polynomials.

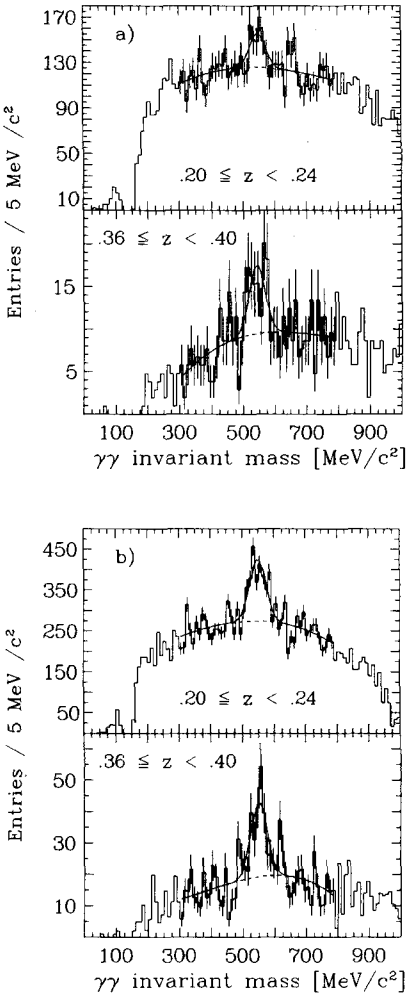

Fig. 3a, b. The $\gamma\gamma$ invariant mass spectra **a** continuum and **b** $\Upsilon(1S) \to 3g$ events in the η mass region after π^0 removal. Selected z bins are shown. The fit results for the η signal (solid line) and the background (dashed line) are superimposed on the data

2.3 *Efficiencies and systematic errors*

The efficiencies of our π^0 and η reconstruction procedures were determined from Monte Carlo studies. With the Lund 6.2/6.3 program versions [8] we simulated the processes $\Upsilon(1S) \to 3g \to hadrons$ and $e^+e^- \to q\bar{q} \to hadrons$. The generated events were passed through a complete detector simulation, where the shower developments of electromagnetically interacting particles were handled by the EGS3 code [9] and the interactions of hadrons were simulated with the GHEISHA6 program package [10]. The Monte Carlo data samples were then analyzed in the same way as our data. The efficiency for each z bin was calculated from the number of π^0 and η mesons obtained from the fits to the invariant mass spectra of the Monte Carlo data compared to the number of generated π^0 and η mesons in the z bin. Figure 4a and b show the π^0 reconstruction efficiencies obtained from the $q\bar{q}$ and the $3g$ Monte Carlo simulations, respectively. Different symbols refer to the two π^0 reconstruction methods. The η efficiencies are plotted in Fig. 5.

The systematic uncertainties in the reconstruction efficiencies and in the π^0 and η yields were studied in some detail. Systematic errors common to the π^0 and η analyses come dominantly from the difference between the two Monte Carlo event generators, the modeling of the calorimeter response, and the tracking chamber performance. These effects contribute a systematic error of 9% on the efficiencies of both analyses.

Systematic uncertainties in the particle yield which are different for the π^0 and η analysis and are specific to either the continuum data or the $\Upsilon(1S)$ data are caused by the following effects. Varying the order of the polynominal function used to model the background

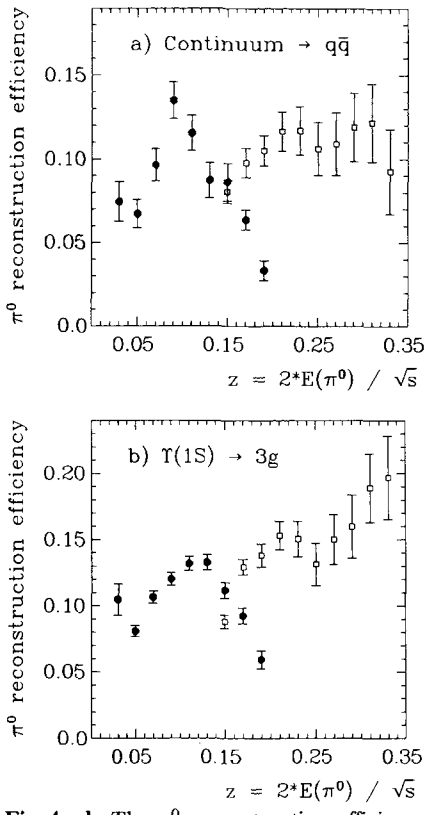

Fig. 4a, b. The π^0 reconstruction efficiency in different z bins for **a** continuum and **b** $\Upsilon(1S) \to 3g$ data. The reconstruction is based on the $\gamma\gamma$ invariant mass (filled circles) or the shower mass method (open squares)

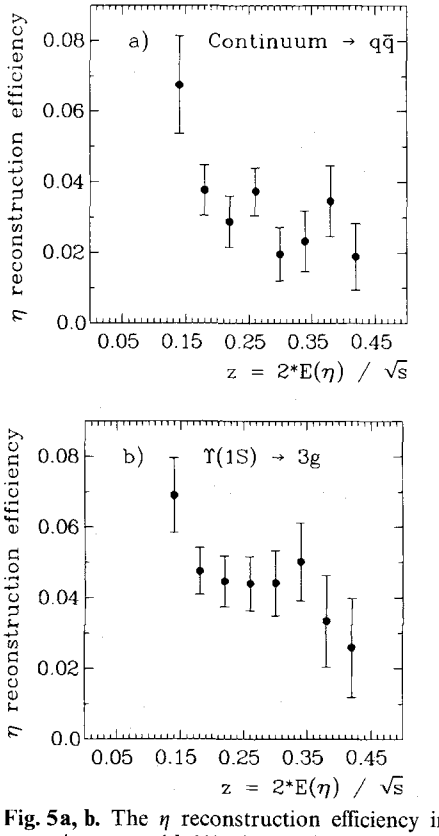

Fig. 5a, b. The η reconstruction efficiency in different z bins for **a** continuum and **b** $\Upsilon(1S) \to 3g$ data

shape of the invariant mass spectra results in a systematic error of 3% and 5% on the π^0 and η yield, respectively. The measurements of particle production in the continuum process $e^+e^- \to q\bar{q}$ is affected by initial state radiation, which can alter the energy spectra of produced light mesons. This effect also reduces the observed mean π^0 and η multiplicities by about 5%. We correct our measured particle spectra for initial state radiation by comparing the z-dependent particle yields for Monte Carlo data generated with and without initial state radiation. This correction procedure adds a systematic uncertainty of 2% for the continuum analysis. Furthermore, the measurement of the particle yields for the continuum data is affected by background from τ-pair events. From the hadronic event selection efficiencies and the cross sections for τ-pair and $q\bar{q}$ production we estimate that about 4% of our final selected continuum events are τ-pair events. In the determination of the π^0 yield this effect is partially compensated, since τ-decays lead to final states with π^0 mesons. Note however, that there are no significant τ-decay modes to final states with η mesons. The above effects are estimated to reduce the observed mean π^0 and η multiplicity per continuum event by 2% and 4%, respectively, and are globally taken into account by scaling the corresponding particle spectra. The remaining systematic uncertainty from this correction is 1% for the π^0 and η continuum analysis.

For roughly half of the $\Upsilon(1S)$ data used in this analysis about 15% of the NaI(Tl) crystals showed a nonlinear energy response due to a malfunction in their electronic readout [11]. From a simulation of these nonlinearities we estimate uncertainties in the particle yield of 3% and 1% for the π^0 and η production study, respectively.

An additional uncertainty of the η production analysis arises from the π^0 subtraction procedure. The dependence of the η yield on the π^0 mass cut used in this algorithm was studied by Monte Carlo simulations. The observed systematic variations change the η yield by about 5%.

The various contributions to the systematic error were added in quadrature. For the π^0 analysis we obtain $\sigma_{\text{syst.}}(\pi^0) = \pm 10\%$ and for the η analysis $\sigma_{\text{syst.}}(\eta) = \pm 12\%$.

3 Results and discussion

3.1 Inclusive energy spectra

We correct the observed π^0 and η yield found in each z-bin for the particle reconstruction efficiency, initial state radiation, τ-background, and for the effect of low multiplicity hadronic events which are rejected by our hadronic event selection algorithm. The inclusive particle spectra are then obtained by dividing the corrected number of π^0 and η mesons in each z by the the number of hadronic events N_{ev} and by the particle velocity $\beta = pc/E$. N_{ev} denotes the number of observed $q\bar{q}$ or $\Upsilon(1S) \to 3g$ events depending on whether the particle spectra of the continuum or the $\Upsilon(1S)$ data sample are

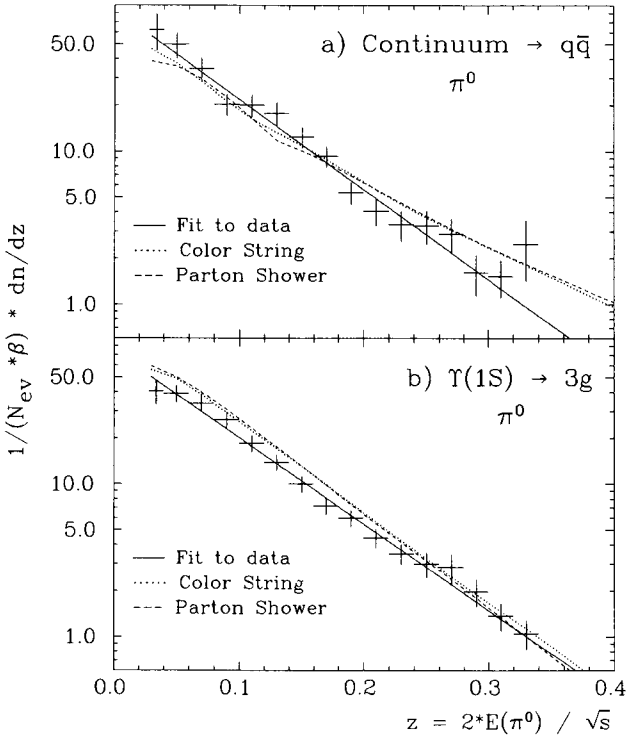

Fig. 6a, b. The inclusive π^0 energy spectra for **a** continuum and **b** $\Upsilon(1S) \to 3g$ data. Statistical and systematic errors are added in quadrature. The fit results described in the text are indicated by solid lines. Also shown are the predictions of the color string model (dotted line) and the coherent parton shower model (dashed line)

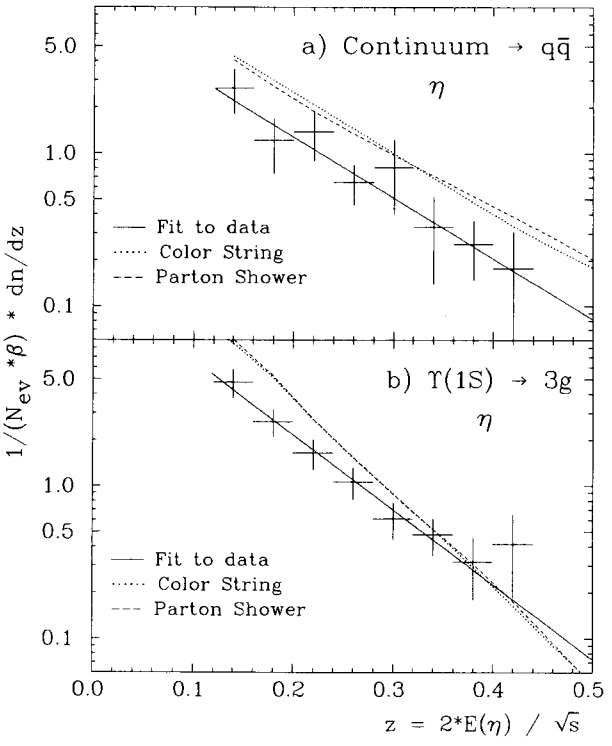

Fig. 7a, b. The inclusive η energy spectra for **a** continuum and **b** $\Upsilon(1S) \to 3g$ data. Statistical and systematic errors are added quadratically. The fit results are superimposed as solid lines. Also shown are the predictions of the color string model (dotted line) and the coherent parton shower model (dashed line)

Table 1. The results of the fits to the inclusive π^0 and η energy spectra. Only the statistical errors are given. The fit function is noted in the table

$F(z)=A\cdot e^{-b\cdot z}$	A	b
π^0: Continuum	84.6 ± 10.2	13.6 ± 0.7
$\Upsilon(1S)\to3g$	74.4 ± 6.0	13.0 ± 0.5
η: Continuum	7.9 ± 3.8	9.1 ± 1.8
$\Upsilon(1S)\to3g$	20.6 ± 6.7	11.3 ± 1.3

studied. We combine the continuum data samples, taken at center-of-mass energies between 9.4 GeV and 10.5 GeV, and analyze them together, since over such a small change in center-of-mass energy no significant variation in the fragmentation behaviour is expected. The luminosity weighted center-of-mass energies of the continuum data samples used for the π^0 and η analyses are 9.58 GeV and 10.24 GeV, respectively. The resulting inclusive energy spectra for π^0 and η production are displayed in Figs. 6 and 7, respectively. For the π^0 spectra the results of both reconstruction methods in the range $0.14 \leqq z \leqq 0.20$ are averaged according to their statistical weights. These spectra were fitted with an exponential function of the form

$$\frac{1}{\beta \cdot N_{ev}} \cdot \frac{dn}{dz} = A \cdot e^{-b \cdot z} \tag{3}$$

with free parameters A and b. The fitted functions are superimposed on the data in Figs. 6 and 7, and the fit results are summarized in Table 1.

Inclusive π^0 and η energy spectra were calculated using the program of [8] on the basis of the Lund color string model [2] and the coherent parton shower model [3]. The measured π^0 energy spectra are compared with the predictions of both models in Fig. 6. Within errors the observed π^0 spectrum for continuum data is in agreement with both models. For the $\Upsilon(1S)$ data the measured π^0 yields at low z values are below the model predictions. The agreement between the measured inclusive η spectra and the predictions based on the two fragmentation models is less satisfactory. For the continuum data (Fig. 7a) the predictions of both models are above our data points and the predicted η spectra in direct $\Upsilon(1S)$ decays (Fig. 7b) are somewhat steeper than our measured one.

A comparison of our results with those obtained by CLEO [12] and ARGUS [13] for inclusive π^0 production in direct $\Upsilon(1S)$ decays is shown in Fig. 8. The spectra are consistent with each other. Our π^0 spectrum for continuum data can also be compared to measurements performed at other center-of-mass energies by multiplying it by $s \cdot \sigma_{had} = s \cdot R \cdot \sigma_{\mu\mu}$ to convert it into an inclusive production cross section. For R we use our measured value [14] of 3.48 ± 0.16 and $\sigma_{\mu\mu}$ denotes the μ-pair cross section in lowest order QED. The scaled differential cross section for π^0 production in the continuum as obtained by different experiments [13, 15–17] at $\sqrt{s}$ = (5–14) GeV is plotted in Fig. 9. For the η production

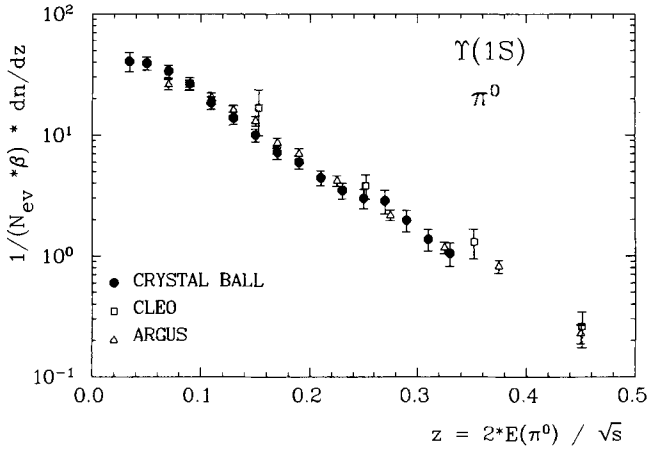

Fig. 8. The inclusive π^0 energy spectra in direct $\Upsilon(1S)$ decays as obtained by Crystal Ball, ARGUS and CLEO

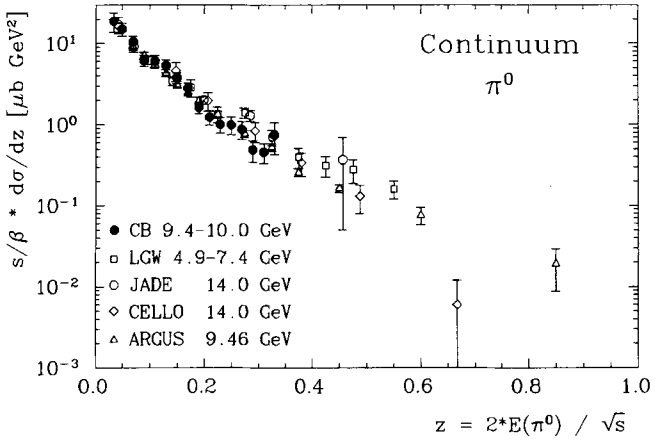

Fig. 9. The scaled differential cross sections for inclusive π^0 production in continuum events as obtained by experiments at $\sqrt{s}$ =(5–14) GeV

in nonresonant e^+e^- annihilation the scaled differential cross section from various experiments [13, 17–19] performed at $\sqrt{s}$ between 9 GeV and 35 GeV is shown in Fig. 10. In both cases good agreement between all measurements is observed. All measured particle rates and inclusive production cross sections together with their combined statistical and systematic errors are listed in detail in Table 3 to Table 6.

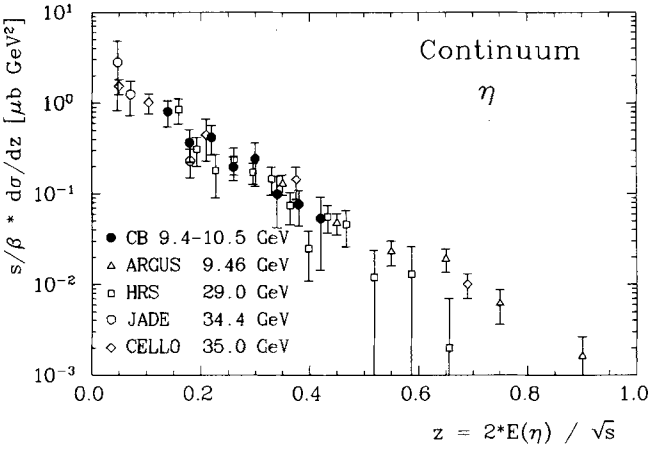

Fig. 10. The scaled differential cross section for inclusive η production in continuum events as obtained by different experiments

3.2 Particle multiplicities

The mean number, $\langle n\rangle$, of π^0 or η mesons per hadronic event, was calculated by integrating the inclusive energy spectra:

$$\langle n\rangle = \int_{z_0}^{1} \frac{1}{N_{ev}} \cdot \frac{dn}{dz} \cdot dz \tag{4}$$

with $z_0 = 2M(\pi^0, \eta)/\sqrt{s}$. Since the spectra were not measured over the full z range the fit results from the previous section have been used in the integral. The extrapolation contributes at most 5% to our derived mean particle multiplicities. The mean number of π^0 mesons per event obtained by this procedure is $\langle n_{\pi^0}\rangle = 3.64 \pm 0.21 \pm 0.36$ for nonresonant $e^+e^- \to q\bar{q}$ events and $\langle n_{\pi^0}\rangle = 3.39 \pm 0.14 \pm 0.34$ for $\Upsilon(1S) \to 3g$ events. From the measured η spectra we obtain $\langle n_\eta\rangle = 0.22 \pm 0.04 \pm 0.03$ for continuum events and $\langle n_\eta\rangle = 0.35 \pm 0.04 \pm 0.04$ for direct $\Upsilon(1S) \to 3g$ decays, where statistical and systematic errors are given separately. For comparison we list in Table 2 together with our results the CLEO [12] and ARGUS [13] results on π^0 and η multiplicities in the $\Upsilon(1S)$ energy region. Within the errors the experiments are in agreement.

The particle multiplicities are also compared in Table 2 with the predictions of the color string and the coherent parton shower fragmentations models. Our

Table 2. Mean multiplicities for π^0 and η mesons in nonresonant $e^+e^- \to q\bar{q}$ events and $\Upsilon(1S) \to 3g$ decays. Statistical and systematic errors are quoted. For comparison the results of the ARGUS and CLEO experiment are given. The predictions of the color string and the coherent parton shower fragmentation models are also listed

Multiplicity $\langle n\rangle$	Crystal Ball	ARGUS	CLEO	Color string	Parton shower
π^0: Continuum	$3.64 \pm 0.21 \pm 0.36$	$3.22 \pm 0.07 \pm 0.31$	3.0 ± 0.7	3.6	3.5
$\Upsilon(1S) \to 3g$	$3.39 \pm 0.14 \pm 0.34$	$3.97 \pm 0.23 \pm 0.38$	5.2 ± 1.8	4.2	4.3
η: Continuum	$0.22 \pm 0.04 \pm 0.03$	$0.19 \pm 0.04 \pm 0.04$	–	0.44	0.42
$\Upsilon(1S) \to 3g$	$0.35 \pm 0.04 \pm 0.04$	$0.40 \pm 0.14 \pm 0.09$	–	0.57	0.59

Table 3. Inclusive π^0 spectrum in the continuum ($\sqrt{s}$= (9.4–10.0) GeV)

z	$\frac{1}{N_{ev}\beta}\frac{dn_{\pi^0}}{dz}$	$\frac{s}{\beta}\frac{d\sigma}{dz}$ (μb GeV^2)
0.028–0.040	62.3 ±16.7	18.8 ±5.1
0.04 –0.06	49.9 ± 9.5	15.1 ±2.9
0.06 –0.08	34.7 ± 5.9	10.5 ±1.8
0.08 –0.10	20.3 ± 3.2	6.14±0.98
0.10 –0.12	20.1 ± 3.3	6.08±1.00
0.12 –0.14	17.7 ± 3.2	5.34±0.98
0.14 –0.16	12.5 ± 1.9	3.77±0.58
0.16 –0.18	9.3 ± 1.4	2.81±0.43
0.18 –0.20	5.38± 0.88	1.63±0.27
0.20 –0.22	4.08± 0.81	1.23±0.24
0.22 –0.24	3.33± 0.74	1.00±0.22
0.24 –0.26	3.27± 0.80	0.99±0.24
0.26 –0.28	2.88± 0.73	0.87±0.22
0.28 –0.30	1.62± 0.48	0.49±0.15
0.30 –0.32	1.52± 0.41	0.46±0.12
0.32 –0.34	2.47± 1.05	0.74±0.32

Table 4. Inclusive η spectrum in the continuum ($\sqrt{s}$= (9.4–10.5) GeV)

z	$\frac{1}{N_{ev}\beta}\frac{dn_{\eta}}{dz}$	$\frac{s}{\beta}\frac{d\sigma}{dz}$ (μb GeV^2)
0.12–0.16	2.66±0.86	0.80 ±0.26
0.16–0.20	1.21±0.48	0.37 ±0.14
0.20–0.24	1.39±0.50	0.42 ±0.15
0.24–0.28	0.65±0.19	0.20 ±0.06
0.28–0.32	0.81±0.41	0.24 ±0.12
0.32–0.36	0.33±0.19	0.099±0.057
0.36–0.40	0.26±0.11	0.077±0.032
0.40–0.44	0.18±0.13	0.054±0.039

Table 5. Inclusive π^0 spectrum in direct $\Upsilon(1S)$ decays

z	$\frac{1}{N_{ev}\beta}\frac{dn_{\pi^0}}{dz}$
0.028–0.04	40.6 ±7.3
0.04 –0.06	39.1 ±4.8
0.06 –0.08	33.8 ±4.0
0.08 –0.10	26.5 ±3.1
0.10 –0.12	18.5 ±2.2
0.12 –0.14	13.8 ±1.7
0.14 –0.16	10.0 ±1.2
0.16 –0.18	7.16±0.86
0.18 –0.20	5.98±0.76
0.20 –0.22	4.43±0.62
0.22 –0.24	3.49±0.52
0.24 –0.26	3.00±0.55
0.26 –0.28	2.85±0.63
0.28 –0.30	1.98±0.40
0.30 –0.32	1.37±0.28
0.32 –0.34	1.05±0.23

Table 6. Inclusive η spectrum in direct $\Upsilon(1S)$ decays

z	$\frac{1}{N_{ev}\beta}\frac{dn_{\eta}}{dz}$
0.12–0.16	4.78±1.00
0.16–0.20	2.64±0.54
0.20–0.24	1.64±0.36
0.24–0.28	1.06±0.25
0.28–0.32	0.61±0.16
0.32–0.36	0.48±0.13
0.36–0.40	0.32±0.14
0.40–0.44	0.42±0.23

measured π^0 multiplicity for the continuum data is in good agreement with both models, while for $\Upsilon(1S)$ data we obtain a π^0 multiplicity two standard deviations below the model predictions. The measured η multiplicities for both samples are smaller than those expected from these models, but show the expected trend of a larger multiplicity in $\Upsilon(1S)\to 3g$ events compared to continuum events.

In the Peterson-Walsh fragmentation model [4] one qualitatively expects the ratio $\langle n_\eta\rangle/\langle n_{\pi^0}\rangle$ to be larger in gluon fragmentation compared to quark fragmentation. We obtain:

$$\frac{\langle n_\eta\rangle}{\langle n_{\pi^0}\rangle}=0.10\pm0.02 \quad (\Upsilon(1S)\to 3g),$$
$$\frac{\langle n_\eta\rangle}{\langle n_{\pi^0}\rangle}=0.06\pm0.02 \quad \text{(Continuum)}. \qquad (5)$$

This shows the trend expected by Peterson and Walsh, but the effect is not very significant due to the large errors. They give a quantitative prediction for quark and gluon jets of energy 10 GeV: the number of η mesons with a scaled energy $z\geqq 0.3$ is expected to be in the range (0.11–0.31) per gluon jet, while it is predicted to be 0.05 per quark jet. The relatively wide range of the predicted η yield is due to theoretical uncertainties in the ratio between vector mesons and pseudoscalars and in the primordial fragmentation function for gluon jets. If these predictions are also valid at lower jet energies, one expects an enhancement of η production in $\Upsilon(1S)\to 3g$ events compared to continuum events by a factor between three to nine. We obtain for the mean number of η mesons per event with scaled energy $z\geqq 0.3$

$$\langle n_\eta\rangle(z\geqq 0.3)=0.059\pm0.015 \quad (\Upsilon(1S)\to 3g),$$
$$\langle n_\eta\rangle(z\geqq 0.3)=0.053\pm0.018 \quad \text{(Continuum)}. \qquad (6)$$

A significantly higher η multiplicity in $\Upsilon(1S)\to 3g$ decays compared to continuum production as expected by this model is not observed.

4 Conclusions

The production of π^0 and η mesons in hadronic events has been studied using the Crystal Ball detector. The inclusive energy spectra of these light mesons and their mean multiplicities were measured for direct $\Upsilon(1S)$ decays and for nonresonant e^+e^- annihilation events.

In the measured range $0.02 \leqq z \leqq 0.34$ the π^0 spectra are reasonably well described by the Lund color string and the coherent parton shower fragmentation models, although for the $\Upsilon(1S) \to 3g$ decays the observed mean multiplicity is two standard deviations below the expectations. The measured η spectra for continuum events and $\Upsilon(1S)$ decays are below the model predictions. In direct $\Upsilon(1S)$ decays a harder η spectrum compared to the model expectations is observed. Our scaled differential cross sections for π^0 and η continuum production are in good agreement with other experimental results obtained over a wide range of center-of-mass energies.

Further, we have studied our measured multiplicities in the light of the predictions of Peterson and Walsh. We observe no significant difference in the π^0 to η meson production ratio between quark and gluon fragmentation.

Acknowledgments. We would like to thank the DESY and SLAC directorates for their support. This experiment would not have been possible without the dedication of the DORIS machine group as well as the experimental support groups at DESY. The visiting groups thank the DESY laboratory for the hospitality extended to them. Z.J., B.M., B.N., and G.N. thank DESY for financial support, E.D.B., R.H., and K.S. have benefited from financial support from the Humboldt Foundation. K. Königsmann acknowledges support from a Heisenberg fellowship.

References

1. X. Artru, G. Mennessier: Nucl. Phys. B70 (1974) 93; X. Artru: Phys. Rep. 97 (1983) 147; A. Bassetto et al.: Phys. Rep. 100 (1983) 201; A. Bassetto et al.: Nucl. Phys. B163 (1980) 477; R.D. Field, S. Wolfram: Nucl. Phys. B213 (1983) 65; T.D. Gottschalk: Nucl. Phys. B214 (1983) 201
2. B. Andersson et al.: Phys. Rep. 97 (1983) 31
3. B.R. Webber: Nucl. Phys. B238 (1984) 492; G. Marchesini, B.R. Webber: Nucl. Phys. B238 (1984) 1
4. C. Peterson, T.F. Walsh: Phys. Lett. B91 (1980) 455
5. K. Wachs et al.: Z. Phys. C – Particles and Fields 42 (1989) 33; K. Wachs: Ph.D. Thesis, University of Hamburg, DESY-F31-88-01 (1988), unpublished
6. Ch. Bieler: Ph.D. Thesis, University of Hamburg, DESY-F31-89-01 (1989), unpublished
7. P. Schmitt et al.: Z. Phys. C – Particles and Fields 40 (1988) 199; R.A. Lee: Ph.D. Thesis, Stanford University, SLAC-282 (1985), unpublished; R.L. Walker: Proceedings of Summer Institute on Particle Physics, July 29–August 10, 1974, SLAC-179 (volume II), 1 (1974)
8. T. Sjöstrand: Comp. Phys. Comm. 39 (1986) 347; T. Sjöstrand, M. Bengtsson: Comp. Phys. Comm. 43 (1987) 367; For color string fragmentation we use the Lund 6.2 version and for parton shower fragmentation the Lund 6.3 program
9. R. Ford, W.R. Nelson: SLAC-210 (1978) unpublished
10. H. Fesefeldt: Aachen preprint, PITHA 85/02 unpublished
11. S.T. Lowe: Ph.D. Thesis, Stanford University, SLAC-307 (1986), unpublished
12. S. Behrends et al.: Phys. Rev. D31 (1985) 2161
13. H. Albrecht et al.: Z. Phys. C – Particles and Fields 46 (1990) 15
14. Z. Jakubowski et al.: Z. Phys. C – Particles and Fields 40 (1988) 49
15. D.L. Scharre et al.: Phys. Rev. Lett. 41 (1978) 1005
16. H.J. Behrend et al.: Z. Phys. C – Particles and Fields 20 (1983) 207
17. W. Bartel et al.: Z. Phys. C – Particles and Fields 28 (1985) 343
18. H.J. Behrend et al.: Z. Phys. C – Particles and Fields 47 (1990) 1
19. S. Abachi et al.: Phys. Lett. B205 (1988) 111